# Geolocation and Stereo Height Estimation Using TerraSAR-X Spotlight Image Data

K. Eldhuset, and D. J. Weydahl

***Abstract*—We have studied the geographic position of several high-resolution spotlight TSX images by investigating the location of deployed radar corner reflectors. Results show that the geolocation accuracy is better than the resolution cell in both azimuth and range directions. The same corner reflectors as well as distinct points on buildings are used to estimate the absolute height from stereo viewing spotlight TSX images to within a few decimeters accuracy.**

***Index Terms*—satellite, synthetic aperture radar, geographic position accuracy, stereo height, corner reflector**

## I. Introduction

The German TerraSAR-X (TSX) satellite platform was launched in 2007. The major sensor onboard is an X-band synthetic aperture radar (SAR) system capable of acquiring data using several imaging modes [1]. The best spatial resolution of 1 meter is obtained with the spotlight mode. The TSX spotlight mode is an advanced SAR imaging mode where the raw data have been focused to single-look complex images in zero-Doppler coordinates [2]. The TSX satellite has a relatively short revisit time of only 11 days. This, together with its radar antenna steering capability, makes it possible to acquire high-resolution SAR data over the same geographic area on the Earth surface within a few days interval.

The geolocation accuracy of pixels within a satellite SAR scene is strongly linked to the attitude and orbit accuracy of the satellite, as well as the SAR processing itself. The initial calibration campaign of TerraSAR-X gave excellent results in this respect, with orbit accuracies approaching 5 cm [3]. Therefore, it is interesting to investigate further if it is possible to achieve SAR image geolocation accuracies well below the resolution cell: i.e. at the centimeter scale.

An overview of TerraSAR-X processing and accompanying products can be found in [4]. There are several levels of satellite orbit accuracies. The best accuracy is achieved using the science orbits. In [5] the influence of atmospheric path delay on the geolocation accuracy was thoroughly investigated. Recently, image pixel location accuracies in the centimeter scale in range have been reported after fine-tuning some of the correction algorithms [6, 7]. Despite these facts, there will still be challenges regarding geolocation accuracy of *orthorectified* SAR images: the geolocation accuracy will depend strongly on the quality of the digital elevation model used in the orthorectification process [8].

In general, if there are well-defined structures that are clearly visible in a pair of TSX images acquired with different radar beam incidence angles, we may use the stereo SAR technique to estimate elevation heights at these points within the SAR image [9]. Investigations have been done with respect to generating digital elevation models (DEMs) from TSX data [10]. Results gave an overall DEM accuracy (LE 90) of around 9 meters when using 10 meters grid spacing. Another study compared the geolocation of certain well defined ground points with the TSX image data using both same-side and opposite side stereo spotlight acquisitions [11]. Here, they achieved a geolocation accuracy of retrieved 3D points in a range between 1 and 1.5 meters.

Deployed corner reflectors can be seen from different incidence angle positions. We will therefore use the measured positions of such corner reflectors to validate the geographic position accuracy of the TSX spotlight image products. At the same time, we will also use our own software to estimate the absolute elevation height at these corner reflector points.

First, we describe our TSX data set in Section II. Then we explain how we use the deployed corner reflectors and how they are positioned using a differential GPS system in Section III.A. In Section III.B we give a short description of our pixel location algorithm and stereo height estimator, and how we use these algorithms together with the TSX data set and corner reflectors to estimate geographical positions in both plane and height from image pixel locations (azimuth and range) within the SAR scene.

In Section IV.A we use the ENVI/SARscape software to verify the position accuracy of corner reflectors. In Section IV.B we minimize the difference of GPS positions and positions estimated with our pixel location algorithm to find azimuth and range corrections. The range corrections will validate the ionospheric and atmospheric path delay given in the accompanying TSX product header. In Section IV.C we validate the TerraSAR-X product header geographic positions. In Section IV.D we improve the pixel location accuracy by finding an azimuth correction from each scene individually. We also minimize the difference of GPS positions and

Manuscript received March 31, 2011. (This work was supported by Norwegian Defence Research Establishment).

Knut Eldhuset is with Norwegian Defence Research Establishment, Land and Airsystems Division, PO Box 25, 2027 Kjeller, Norway (phone: +47-63-807478; fax: +47-63-807212; e-mail: knut.eldhuset@ffi.no).

Dan Johan Weydahl is with Norwegian Defence Research Establishment, Land and Airsystems Division, PO Box 25, 2027 Kjeller, Norway (e-mail: dan-johan.weydahl@ffi.no).


DOI til publisert versjon / DOI to published version: 10.1109/TGRS.2011.2160951

estimated pixel positions using the individual azimuth corrections in each scene.

## II. Data Set

We have several TerraSAR-X high-resolution spotlight images available from two test sites in Norway. Four of them were acquired in August 2008, while three of them were acquired in June/July 2009 using the 300 MHz range bandwidth option, instead of the default 150 MHz bandwidth. Two of the images are shown in Fig.1. The images were all processed to single look complex (SSC) products by the German Aerospace Center (DLR). See Table I. All the images have an SSC pixel spacing of 0.86 m in azimuth direction, and a slant range pixel spacing of 0.91 m and 0.45 m for the 150 MHz and 300 MHz bandwidths respectively. The data sets were processed with science orbits. This gives satellite orbit positions to a few centimeters accuracy [3].

The TSX image products are accompanied by a special header file <GEOREF.xml>. This header file contains estimated geographic coordinates (latitude/longitude) for a grid of image pixels within the scene, as well as numbers for the expected ionospheric and atmospheric range path delay for the same scene [4]. The path delay corrections, the grid of geographic positions, the sensor system parameters (e.g. satellite orbit data,- which are located in the main <.xml> header file accompanying the TSX image file) and the SAR processing parameters, can be used together to estimate geoposition accuracies within the TSX image.

## III. Methodology

The aim is to estimate the geographic position accuracy of the TSX spotlight images. This is done by using deployed radar corner reflectors together with a dedicated SAR image pixel position algorithm developed at the Norwegian Defence Research Establishment (FFI). This allows us to obtain a quantitative estimate of the geolocation accuracy in the TSX spotlight test data set.

### *A. Radar Corner Reflectors*

Several radar corner reflectors were deployed within the area of the acquired TSX scenes. The trihedral triangular radar corner reflectors vary in size from 0.33 m to 1.8 m (short side length). The large corner reflectors are also used for other space borne SAR sensors with coarser resolution.

The corner reflectors were oriented to give a strong SAR backscatter in either ascending or descending satellite passes for polar orbiting SAR sensors. The larger radar reflectors were tilted to maximize the radar backscatter at radar incidence angles around 40 degrees, while the smaller reflectors were tilted to give an optimum signal strength for the specific TSX acquisitions in question.

The positions of the radar corner reflectors were measured in mid 2009 with a differential GPS (static) system. The GPS raw data were fed into the Canadian PPP-On-Line positioning service system [12] to produce estimated positions with a few centimeters accuracy in plane and height for two reference stations using the ITRF05 reference system. The other corner reflectors were measured by static GNSS in a network of vectors. The ITRF05 system can be considered the same as WGS84 (measurements may differ by a few centimeters). TSX products are available in either reference system.

### *B. Pixel Location and Stereo Height Algorithm*

FFI has developed a high-precision pixel position algorithm ("FFI_pix_pos") for satellite SAR images [13, 14]. The algorithm uses a two-step approach to solve a set of non-linear equations. We refer to [13, 14] for the details. Based on a selected pixel position within the satellite SAR image (range and azimuth pixel number), the algorithm calculates the geodetic latitude and longitude position of that pixel. The algorithm was first used for ERS [15] and Radarsat-1 SAR images, and was later adapted to also work for Radarsat-2 and TSX images where interpolation in the state vectors are performed using Chebyshev polynomials. The Doppler frequency in Eq. 2 in [14] is set to zero for a zero-Doppler product. This is indeed done here when working with our TSX image products, since TSX raw data is focused to the zero-Doppler azimuth time domain (see explanation in section IV.B in [4]).

The geographic positions of the radar corner reflectors seen in the TSX scenes were estimated using the following steps:

- Several TSX spotlight scenes were acquired at different look angles.
- Four corner reflectors are visible in each of these TSX scenes.
- The center point position of each corner reflector was estimated to sub-pixel level by interpolating the peak position.
- Finally, we used four different methods (see Sections IV.A, IV.B, IV.C and IV.D) to estimate the geographic position of the corner reflectors.

We combine two algorithms developed at FFI: a pixel position algorithm, and a stereo SAR height estimator. With these algorithms, it is possible to identify the location of a common ground control point (e.g. a corner reflector) seen in two SAR images, and let the software estimate the absolute height (in our case; the height above the WGS84 ellipsoid) of this particular point. The positions $(X_1, Y_1, Z_1)$ and $(X_2, Y_2, Z_2)$ of the two selected pixels are estimated by "FFI_pix_pos" in two images as if the common point were on the ellipsoid. For each of the positions $(X_1, Y_1, Z_1)$ and $(X_2, Y_2, Z_2)$ there is a vector $\vec{N}_1$ and $\vec{N}_2$ perpendicular to the ellipsoid. Each of the vectors and each of the satellite positions define a plane. Then the algorithm moves along two

Dette er en postprint-versjon / This is a postprint version.
DOI til publisert versjon / DOI to published version: 10.1109/TGRS.2011.2160951

circles from the points $(X_1, Y_1, Z_1)$ and $(X_2, Y_2, Z_2)$ in both planes until the distance between the circles is minimized. The distance from the closest approach down to the ellipsoid is taken to be the estimated SAR stereo height.

## IV. Results

### A. Visual Inspection of Corner Reflector Positions after Image Geocoding

First, we verified the position accuracy of some of the deployed radar corner reflectors by visual inspection of geocoded TSX images. The geocoding was performed with ENVI/SARscape software to a WGS84 UTM zone 32 map projection with grid spacing of 2 meters. The geocoding was carried out in two ways:

- Applying no ionosphere/atmospheric corrections.
- Applying the ionosphere/atmospheric corrections found in the <GEOREF.xml> file.

All the corner reflectors are easily seen in the amplitude version of the single-look-complex (SSC) TSX spotlight images. Their initial positions are clearly not quite correct, see Table II where one corner reflector close to the Kjeller airport (see Fig. 2) is shown for four TSX spotlight images.

Slant range corrections corresponding to both the ionospheric ("averaged TECU") and atmospheric ("hydrostatic") range path delay are estimated by DLR and inserted into the accompanying <GEOREF.xml> file as two numbers. The number for the atmospheric path delay is normally in the meter range, while the corrections for the ionosphere are in the centimeter range. The total slant range path corrections (atmosphere + ionosphere) varied from 2.5 m to 3.8 m for four of the TSX images in question (see second column in Table II). The azimuth timing correction was set by DLR to a fixed value of -0.00018 seconds (corresponding to 1.27 m) for all the present scenes. We also find this number in the <GEOREF.xml> file.

We may now edit these corrections into the main TSX header files *before* carrying out the image geocoding step in ENVI/SARscape. The result is a much better match of the corner reflector positions at the Kjeller airport which can be seen in the SAR images in the right most column in Table II. From visual inspection, we will consider the corrected position accuracy to better than the pixel size (here: 2 meters).

### B. Estimating the Geographic Position Accuracy from Corner Reflector Positions

Several of the corner reflectors deployed around Lillestrøm city and Oslo city were used to estimate the geoposition of the TSX image. We used two scenes with 4 reflectors and one scene with three reflectors acquired over Oslo in June-July 2009, and four scenes with four reflectors acquired over Lillestrøm in August 2008 (see Table I). These add up to 27 corner reflector points for our analysis. We applied the "FFI_pix_pos" routine to the TSX data and minimized the difference of the measured corner reflector GPS positions and "FFI_pix_pos" positions by adjusting the azimuth time and range. The results are shown in Table III. The standard deviation in longitude is quite small (0.42 m) while the standard deviation in latitude is almost three times larger (1.12 m). The overall pixel position estimate led to a slant range correction that corresponded to a 0.1 m difference as compared to the <GEOREF.xml> values:

$$\text{RangeCorr(FFI)} = \text{RangeCorr(GEOREF)} + 0.1 \text{ m}$$

This means that the ionosperic and atmospheric corrections in the <GEOREF.xml> file are very accurate in the scenes we have tested. We did not observe a range bias as reported in [5], where they indicate that their range error offset between 50 cm and 70 cm may be caused by an SWST (Sampling Window Start Time) bias.

In azimuth we estimated a very small azimuth correction (0.00002 s) which is a factor ten less than the value provided in the <GEOREF.xml> file (-0.00018 s). However, the standard deviation is quite large (1.12 m) which indicates a variable azimuth error position in the scenes. This is investigated further in Section IV.D.

### C. Validating the GEOREF Position Accuracies

The <GEOREF.xml> file contains geographic positions (latitude and longitude) for a set of image grid points (range and azimuth pixel number of the TSX scene). These geographic positions are obtained and edited by DLR after first implementing the azimuth timing and path delay corrections. In other words, the positions found in the <GEOREF.xml> file should be the best possible.

We validated the <GEOREF.xml> positions with respect to our corner reflector positions. All together, we had 27 radar corner reflector positions from seven different TSX spotlight scenes, see Table I. At each corner reflector position, we also had differential GPS measurements that subsequently were used to validate the <GEOREF.xml> geographic positions.

Results are given in Table IV. We notice that the mean geographic position error is less than 0.4 m in both latitude and longitude directions, and one standard deviation is around 0.5 meter.

### D. Geoposition Improvements by New Doppler Estimates

The TSX spotlight scenes are processed to zero Doppler. However, after investigating several TSX spotlight images together with their header information, we discovered that there is a small geographic position offset in the azimuth direction of the processed SAR images. Hereafter, we will call this offset a *residual Doppler*. The residual Doppler was estimated in the following way: The geographic latitude, longitude and reference height of a given pixel in the

Dette er en postprint-versjon / This is a postprint version.
DOI til publisert versjon / DOI to published version: 10.1109/TGRS.2011.2160951

<GEOREF.xml> file was converted to (X,Y,Z) in a rotating earth system. This point, together with the state vectors of the satellite, was then used in Eqs. 2 and 3 in [14] to estimate the Doppler frequency. Ideally, a pixel in the zero-Doppler product should be placed at zero Doppler frequency.

Prior to using the "FFI_pix_pos" program, we corrected the slant range path delay by the numbers (ionospheric and atmospheric corrections) found in the <GEOREF.xml> file. *No additional* azimuth and range corrections were used as input here. The residual Doppler values varied from 0.6 to 1.5 Hz in the scenes we tested when no azimuth time correction was used as input. The residual Doppler number was then used as input to the "FFI_pix_pos" program instead of zero Doppler. In this manner, we were able to estimate the azimuth time *individually* for every TSX scene. Finally, the estimated geographic positions (latitude and longitude) are compared to the measured GPS corner reflector positions. The result is a better geographic position accuracy as well as a smaller standard deviation, see results in Table V in the left column.

Finally, we minimized the difference of the GPS positions and "FFI_pix_pos" using our estimated residual Doppler as input. This result is given in the right column in Table V, with a range correction of 0.1 m and an azimuth correction of only -0.000027 s (which corresponds to a distance less than 0.2 m). We notice that the standard deviation in latitude (which is roughly in the azimuth direction) is reduced to 0.3 m as compared to 0.38 m in the left column.

Assuming that these results are valid for other TSX spotlight scenes, we may be able to *obtain decimeter geoposition accuracies* by using data from the accompanying <GEOREF.xml> file in combination with our own "FFI_pix_pos" software, *without using any additional ground control point*, which is a significant contribution towards providing improved geolocation accuracies automatically.

### *E. Height Estimation of Corner Reflectors*

Radar corner reflector heights from Lillestrøm were estimated by applying different stereo combinations of the four TSX scenes. Results are given in Tables VI and VII. We see from both tables that the standard deviations of the height estimations for the corner reflectors are a few decimeters. The WGS84 system and ITRF'05 are almost equal within a few centimeters, as also assumed in [5].

### *F. Results from Building Height*

We did also try to estimate the height of some large buildings. However, we notice that building structures have to be visible in both SAR images involved in the stereo height estimation. Of course, it is not obvious that there will be numerous matching points originating from the same object within an urban environment. In our study here, we have therefore selected matching points with great care in a semi-manual way. Picking out matching structures in an automatic manner from a set of two, three or four stereo SAR scenes will be subject for a separate algorithm development in a future study.

The present TerraSAR-X images showed some very clear bright backscatter points from a large flat roof in Lillestrøm, see Fig. 4. The bright points can be attributed to the roof window corners of the Norwegian Trade Fair building, see photos in Fig. 3. These square roof windows extend only 30-40 cm above the flat roof surface. We estimated the absolute height of this roof with respect to the WGS84 ellipsoid by selecting matching roof window points in the four TSX images in Table I, see Fig. 4. From these four TSX images, we produced six combinations of pairs, yielding height estimates of 156.7 m, 156.9 m, 156.9 m, 157.3 m, 157.1 m and 156.8 m above the WGS84 ellipsoid. The *average absolute height* of these six estimates is 157.0 m. When taking the local geoid height into account (38.5 m), this means that the height of the roof is estimated to 118.5 m above sea level. In comparison, registered building plans show a cornice height of 118.4 m. From field observations of the roof, it is reasonable to assume that the TSX radar phase center of the roof window is indeed close to the cornice height itself.

We also investigated the roof height from a second building: a large sports hall, see Fig. 5. Using the same stereo-SAR method as above, we estimated a roof height of 21.1 meters above the surrounding sports fields. In this case, the building survey map indicates a roof height of 23 m above the surrounding ground. The difference is nearly 2 meters or approximately 8%. However, we will try to give some reasons for this mismatch. First, there may be differences in what is defined as the level for the ground: the present sports fields may have a different elevation compared to what was defined in the original building plan. However, we assume that this is in the decimeter scale, and does not explain all the 1.9 m difference. Another factor is the radar signal itself. The stereo-SAR estimate indicates that the SAR signal observes a *lower* roof structure. Is this reasonable? This sports hall has ten large steel arches that are "visible" in the SAR-image and that are used when we estimate the roof height based on the stereo-SAR technique (see Fig. 5). These metal arches are interconnected with a special light sandwich structure roof, see photos in Fig. 5. A possibility is that the radar signal partly penetrates the upper sandwich roof structure, and that the SAR backscatter comes from the steel arches embedded inside the roof structure itself. An extra radar beam path length will thus in turn lead to a "lower" scattering origin, as we notice in our results. Finally, uncertainties in the image based matching of the strong radar returns from the arches seen in the different TSX images, could also lead to a vertical offset.

We conclude that it is sometimes difficult to know exactly from which building construction elements the SAR reflections originate. Certainly, some additional knowledge about the object would help us to determine the height more precisely. Alternatively, a mismatch of an expected elevation height may add some knowledge regarding the material/surface type or even its construction complexity. For the deployed triangular

Dette er en postprint-versjon / This is a postprint version.
DOI til publisert versjon / DOI to published version: 10.1109/TGRS.2011.2160951

radar corner reflectors used in this study however, we can safely assume that the phase center point is in the apex.

## V. Conclusion

Our results show that pixels within the TSX spotlight data sets are very well geolocated. By applying the slant range and azimuth timing correction values that accompany the TSX spotlight image file, it is possible to obtain a geolocation accuracy better than the resolution cell in the geocoding process.

As an initial baseline, we simply compared the geographical positions given in the TSX product file with GPS positions of deployed radar corner reflectors visible in the TSX image. The mean position accuracy was estimated to less than 0.36 m, and with a one standard deviation less than 0.6 m.

A high-precision algorithm has been developed at FFI to estimate the TSX image residual Doppler by using the TSX product file positions together with the ionospheric and atmospheric corrections given in the TSX product file. From these estimates, we were able to achieve image pixel geoposition accuracies close to 0.1 m and with a one standard deviation of 0.38 m when referenced to the deployed radar corner reflectors.

We also used the measured GPS positions of our radar corner reflectors as input to estimate *one* azimuth (-0.00002 s) and *one* range (0.1 m) correction for all our seven TSX spotlight scenes. This yielded an average pixel position accuracy around 0.1 m with a one standard deviation less than 0.3 m.

The high-resolution TSX images give the opportunity to gather information from many fine-detailed man-made and urban objects. Many of these objects may give a strong SAR backscatter at several radar beam incidence angles. This has the potential of collecting numerous common ground control points from the same area. We have shown that it is possible to estimate the absolute elevation height to decimeter accuracy using a stereo SAR approach. This is a promising technique that may be further refined in order to extract the necessary ground control points needed for certain interferometric SAR applications in a more automatic procedure.

Accurate geographic location of TSX image pixels in 3D also opens up for new applications in the domain of man-made feature extraction for high-resolution mapping purposes, as well as providing detailed information for disaster management.

## Acknowledgment

The SAR data from Lillestrøm city were acquired under the TSX AO MTH-0181 project supported by DLR. We like to thank Trond Eiken and Tormod Urke at University of Oslo (Norway), Department of Geography, for carrying out differential GPS measurements. The authors also appreciate the valuable suggestions from the anonymous reviewers.

## References

[1] S. Buckreuss, W. Balzer, P. Muhlbauer, R. Werninghause, and W. Pitz, "The TerraSAR-X satellite project," in *Proc. IGARSS*, Toulouse, France, 2003, vol. 5, pp. 3096-3098.

[2] M. Eineder, N. Adam, R. Bamler, N. Yague-Martinez, and H. Breit, "Spaceborne spotlight SAR interferometry with TerraSAR-X", *IEEE Trans. Geosc. Remote Sensing*, Vol. 47, No. 5, May 2009.

[3] Y.T. Yoon, M. Eineder, N. Yague-Martinez, O. Montenbruck ,TerraSAR-X Precise Trajectory Estimation and Quality Assessment, *Trans. Geosc. Remote Sensing*, Vol. 47, No. 6, June 2009.

[4] H. Breit, T. Fritz, U. Balss, M. Lachaise, A. Niedermeier, M. Vonavka, "TerraSAR-X SAR Processing and Products", *IEEE Trans. Geosc. Remote Sensing*, Vol GRS-48, pp. 727-740, February 2010.

[5] A. Schubert, M. Jehle, D. Small, E. Meier, "Influence of Atmospheric Path delay on the Absolute Geolocation Accuracy of TerraSAR-X High-Resolution Products", IEEE Trans. Geosc. Remote Sensing, Vol GRS-48, pp. 751-758, February 2010.

[6] M. Eineder, X. Cong, C. Minet, T. Fritz, P. Steigenberger, "Towards imaging geodesy – achieving centrimetric pixel localization accuracy with TerraSAR-X", *Proceedings of EUSAR 2010*, Aachen Germany, 7-10 June 2010.

[7] M. Eineder, C. Minet, P. Steigenberger, X. Cong, T. Fritz, "Imaging Geodesy - Toward Centimeter-Level Ranging Accuracy With TerraSAR-X", *IEEE Trans. Geosc. Remote Sensing*, Vol. 49, No. 2, pp. 661-671, February 2011.

[8] W. Koppe, N. Kiefl, S. D. Hennig, and J. Janoth, "Validation of pixel location accuracy of orthorectified TerraSAR-X products", *Proceedings of EUSAR 2010*, Aachen Germany, 7-10 June 2010.

[9] F. W. Leberl, "Radargrammetric image processing", Artech House, 1990.

[10] S. D. Hennig, W. Koppe, N. Kiefl, and J. Janoth, "Validation of radargrammetric digital elevation models (DEMs) generated with TerraSAR-X data", *Proceedings of EUSAR 2010*, Aachen Germany, 7-10 June 2010.

[11] H. Raggam, R. Perko, K. Gutjahr, N. Kiefl, W. Koppe, and S. Hennig, "Accuracy assessment of 3D point retrieveal from TerraSAR-X data sets", *Proceedings of EUSAR 2010*, Aachen Germany, 7-10 June 2010.

[12] http://www.geod.nrcan.gc.ca/products-produits/ppp_e.php

[13] K. Eldhuset, "Accurate attitude estimation using ERS-1 SAR raw data", *Int. Journal Remote Sensing*, Vol. 17, No. 14, pp. 2827-2844, September 1996.

[14] J. C. Curlander, "Location of spaceborne SAR imagery", *IEEE Trans. Geosc. Remote Sensing*, Vol GRS-20, pp. 359-364, July 1982.

[15] K. Eldhuset, "An automatic ship and ship wake detection system for spaceborne SAR images in coastal regions", *IEEE Trans. Geosc. Remote Sensing*, Vol. 34, No. 4, July 1996.

**K. Eldhuset** was born in 1958 and received the cand. scient. degree (M.Sc.) in nuclear physics in 1983 from the University of Oslo and the dr. scient. degree (Ph.D.) in physics/signal processing (1987) from the University of Tromsø. He has been with the Norwegian Defence Research Establishment (FFI) since 1983, working on processing and applications of satellite Synthetic Aperture Radar (SAR) data.

His research interests cover a wide range of topics, including orbit simulation, geolocation, automatic ship detection, SAR/scanSAR processing, INSAR processing, scattering theory, polarimetry, MTI simulations and processing of bi-static SAR data. His results have contributed to numerous national projects, to European defence research projects and to several studies for the European Space Agency. He has developed advanced algorithms for ship and wake detection, and for SAR processing using the Extended Exact Transfer Function (EETF), both of which were developed into commercial products by the Kongsberg Group. While his early work was focused on ERS, ENVISAT and Radarsat-1, his more recent work has focused on polarimetric analysis of Radarsat-2 images and interferometry and stereoSAR using TerraSAR-X and COSMO-SkyMed.

**D. J. Weydahl** received the B.Sc. degree in electronic communication in 1988 and the Dipl.Eng. degree in 1991, both from University of Salford, U.K., and the Ph.D. degree from the University of Oslo in Norway in 1998. He has been a scientist at Norwegian Defence Research Establishment (FFI) since 1989.

His research interests are in satellite image processing, SAR image calibration, multitemporal SAR image change detection and analysis, and SAR interferometry and polarimetry. He has contributed to several international scientific work packages organized through WEAG EUCLID, participated in the European Multisensor Airborne Campaign, been co-investigator of an ESA AO-Tandem project, and been principal investigator for X-SAR/SRTM as well as ENVISAT ASAR and ALOS PALSAR. He is presently principle investigator for Radarsat-2, TerraSAR-X, and Cosmo-SkyMed projects. He is also giving lectures in SAR image analysis at the University of Oslo.

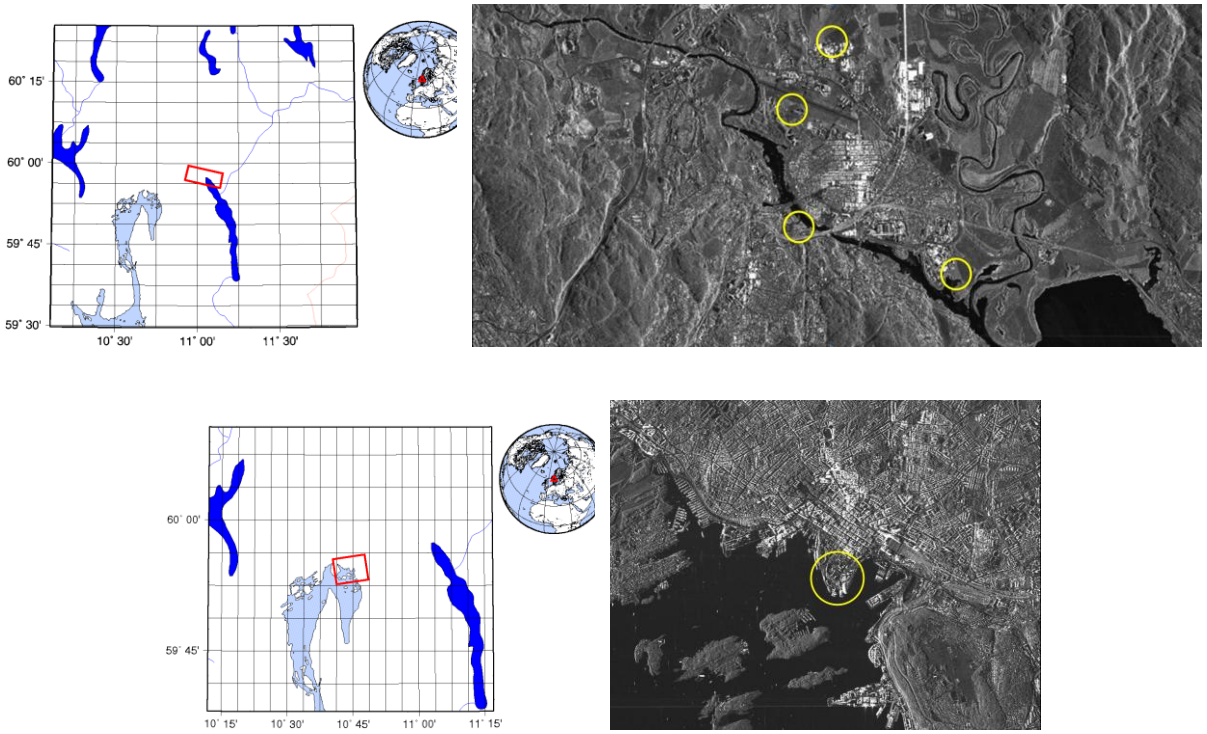


Fig. 1. Map overview and TerraSAR-X browse images from the two test areas in Norway. Lillestrøm city in August 2008 (top), Oslo city in June 2009 (lower). Copyright SAR data: TSX 2008, DLR. Areas with the deployed radar corner reflectors are marked with circles. The one large circle in the bottom image marks the location of several corner reflectors.

Fig. 2. Radar corner reflector at Kjeller airport. Photo: D. J. Weydahl, FFI.

Dette er en postprint-versjon / This is a postprint version.
DOI til publisert versjon / DOI to published version: 10.1109/TGRS.2011.2160951

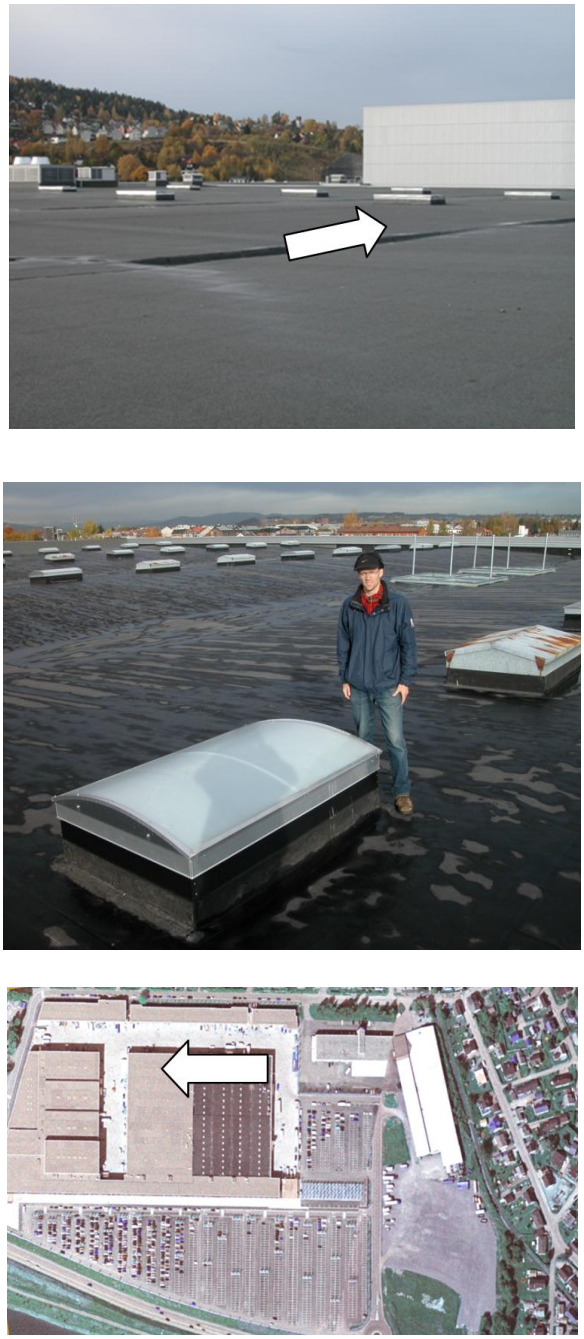

Fig. 3. Norwegian Trade Fair building in Lillestrøm, Norway. Top: Photo of trapdoor windows on the western part of the flat roof structure (D. J. Weydahl, FFI). Middle: Photo of trapdoor windows on the eastern part of the flat roof structure (D. J. Weydahl, FFI). Bottom: Vertical aerial photo taken in June 2003 (B. Fremstad, FFI). White arrows indicate the position of the trapdoor windows used to estimate the height of the flat roof.

Fig. 4. Norwegian Trade Fair building in Lillestrøm, Norway. A subset of the TSX images acquired over Lillestrøm with 54˚ (upper image) and 47˚ (lower image) incidence angles. Note the trapdoor windows on the roof showing up as bright backscatter spots in the SAR images. The spots marked with a white arrow on the western part of the roof are used to estimate the roof height, see also corresponding photo on the very top of Figure 3. Copyright SAR data: TSX 2008, DLR.

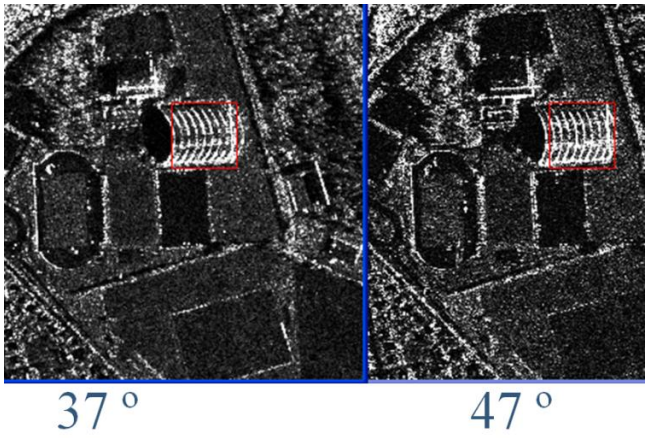


Fig. 5. Sports hall north of Lillestrøm city centre. Top: Two of the TSX images acquired with 37˚ and 47˚ incidence angles. Note the arches that are shown up with bright backscatter in the SAR images. Copyright SAR data: TSX 2008, DLR. Middle and Bottom: Photos of the sports hall with the sandwich roof being mounted (D. J. Weydahl, FFI).

TABLE I
TerraSAR-X spotlight images acquired over two city areas in Norway using ascending or descending satellite pass with varying radar beam incidence angles.

| **Location** | **Date of acquisition** | **Satellite pass** | **Radar beam incidence angle** |
|---|---|---|---|
| Lillestrøm | 16 Aug 2008 | Desc. | 37˚ |
| Lillestrøm | 17 Aug 2008 | Desc. | 54˚ |
| Lillestrøm | 21 Aug 2008 | Desc. | 28˚ |
| Lillestrøm | 22 Aug 2008 | Desc. | 47˚ |
| Oslo | 29 Jun 2009 | Asc. | 49˚ |
| Oslo | 30 Jun 2009 | Asc. | 31˚ |
| Oslo | 11 Jul 2009 | Asc. | 31˚ |

TABLE II
One radar corner reflector at Kjeller airport seen in the four TSX images *before* (third column) and *after* (right most column) applying the radar path delay corrections. The corrections applied here are taken from the accompanying <GEOREF.xml> files. The "cross" marked on top of the corner reflector backscatter, indicates the location of the measured GPS position.

| **TSX radar inc. angle** | **GEORE F slant range corr. [m]** | **Geocoded TSX image without corrections** | **Geocoded TSX image with range and azimuth corrections** |
|---|---|---|---|
| 28° | 2.54 | 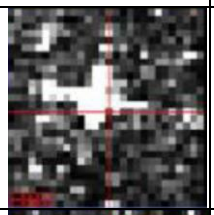 | 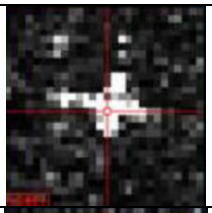 |
| 38° | 2.86 | 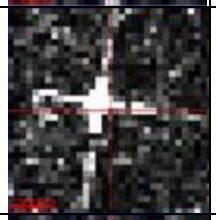 | 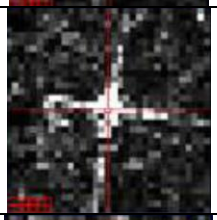 |
| 47° | 3.27 | 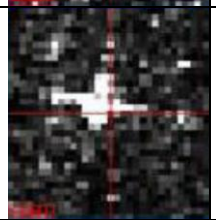 | 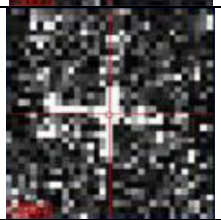 |
| 54° | 3.77 | 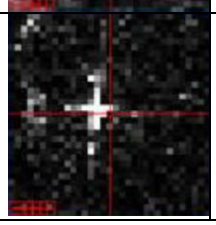 | 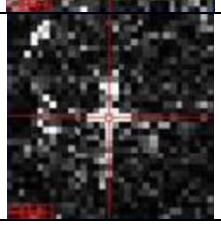 |

Dette er en postprint-versjon / This is a postprint version.
DOI til publisert versjon / DOI to published version: 10.1109/TGRS.2011.2160951

TABLE III
Estimates using 27 radar corner reflector positions found within seven TSX spotlight scenes acquired over Lillestrøm city and Oslo city in Norway in 2008 and 2009 respectively.

| **Parameter** | **27 points (Descending pass & Ascending pass)** |
|---|---|
| Mean error latitude [m] | -0.009 |
| Mean error longitude [m] | 0.35 |
| St. dev. latitude [m] | 1.12 |
| St. dev. longitude [m] | 0.42 |
| Range correction [m] | 0.1 |
| Azimuth correction [s] | 0.00002 |

TABLE IV
Validating the <GEOREF.xml> geographical position accuracies using radar corner reflectors seen in a set of seven different TSX Spotlight scenes acquired in 2008 and 2009 over test two sites Norway.

| **Parameter** | **GEOREF accuracies validated using 27 corner reflector points** |
|---|---|
| Mean error latitude [m] | -0.36 |
| Mean error longitude [m] | -0.20 |
| St. dev. latitude [m] | 0.53 |
| St. dev. longitude [m] | 0.57 |

TABLE V
Geoposition accuracy achieved using the "FFI_pix_pos" routine together with data from the <GEOREF.xml> files.

| **Parameter** | **Geoposition accuracies using the "FFI_pix_pos" program with additional residual Doppler estimates, and compared to 27 corner reflector points** | **Minimizing the difference of corner reflectors DGPS positions and "FFI_pix_pos" using residual Doppler for 27 corner reflector points** |
|---|---|---|
| Mean error latitude [m] | -0.12 | -0.05 |
| Mean error longitude[m] | 0.12 | 0.13 |
| St. dev. latitude [m] | 0.38 | 0.30 |
| St. dev. longitude [m] | 0.24 | 0.24 |
| Range correction [m] | 0.0 (Input) | 0.1 (Output) |
| Azimuth correction [s] | 0.0 (Input) | -0.000027 (Output) |

TABLE VI
Estimated elevation heights from three radar corner reflectors deployed outside Lillestrøm city in Norway. The true value is measured with a differential GPS system (see last row in table). The mean values are estimated from six stereo combinations.

| **TSX scene combination, incidence angle [degrees]** | **Estimated height for corner reflector at Dynea industry area [m]** | **Estimated height for corner reflector at FFI [m]** | **Estimated height for corner reflector at Kjeller airfield [m]** |
|---|---|---|---|
| 47˚ and 54˚ | 144.1 | 150.7 | 140.8 |
| 28˚ and 37˚ | 144.3 | 150.7 | 141.9 |
| 28˚ and 54˚ | 144.4 | 150.8 | 141.7 |
| 28˚ and 37˚ | 144.5 | 150.5 | 141.3 |
| 37˚ and 47˚ | 144.8 | 151.1 | 142.8 |
| 37˚ and 54˚ | 145.3 | 151.0 | 142.0 |
| Mean(St.Dev.)[m] | 144.6 (0.4) | 150.8 (0.2) | 141.8 (0.5) |
| DGPS height [m] | 144.3 | 151.09 | 142.06 |
| Height error [m] | +0.3 | -0.29 | -0.26 |

TABLE VII
Height estimation of four corner reflectors deployed close to Akershus Castle in Oslo during the TSX acquisitions in June/July 2009. Only one stereo image pair is used in this estimation.

| **Reflector ID** | **Stereo height in WGS84 [m]** | **GPS height in ITRF'05 [m]** | **Height error [m]** |
|---|---|---|---|
| # 1 | 46.91 | 47.19 | -0.28 |
| # 2 | 47.36 | 47.64 | -0.28 |
| # 3 | 48.85 | 49.06 | -0.21 |
| # 4 | 48.93 | 49.26 | -0.33 |

Dette er en postprint-versjon / This is a postprint version.
DOI til publisert versjon / DOI to published version: 10.1109/TGRS.2011.2160951